Heat transfer in a 4.1L engine radiator: experimental validation

Transferencia de calor en un radiador de motor 4.1L: validación experimental

Juan Mauricio Trenado Herrera[1] ✉ Crisanto Mendoza Covarrubias[1] Alicia Aguilar Corona[1] Gildardo Solorio Díaz[1]

[1]Facultad de Ingeniería Mecánica, Av. Villa Universidad Morelia, Michoacán, México.

Abstract

Introduction: The thermal performance of internal combustion engines largely depends on the efficiency of their cooling systems. Radiators play a fundamental role in dissipating the heat generated, ensuring the proper functioning of the engine. Analyzing radiator designs using tools such as computational fluid dynamics (CFD) allows for the evaluation of heat transfer and pressure losses—key aspects for understanding and improving the thermal behavior of the system. The geometry of the tubes and fins is a determining factor in this process, as it directly influences both heat dissipation and pressure drop.

Objective: This study aims to analyze heat transfer in a 4.1 L internal combustion engine radiator by combining CFD simulations and experimental validation, in order to evaluate its thermal performance and characterize its behavior under real operating conditions.

Methodology: A CFD model with 9 tubes and 4 rows of fins was used, representing a commercial radiator with three columns of 28 tubes each. The k-ω SST turbulence model was applied, and simulations were performed in ANSYS Fluent. Numerical results were validated with experimental measurements in a test bench, where temperatures, pressures, and flow velocities were recorded.

Results: Experimental validation showed a difference of less than 5.8% compared to the simulation. An 18% improvement in heat transfer and a 12% reduction in pressure drop were achieved. The geometrical arrangement of tubes and fins proved to be a key factor in thermal efficiency, as small modifications can significantly enhance heat dissipation without increasing aerodynamic resistance.

Conclusions: The validated CFD model accurately predicts the thermal performance of the radiator under specific operating conditions. However, the study presents certain limitations, such as geometric simplifications and the choice of turbulence model, which can be improved in future research. It is recommended to explore the use of advanced materials and hybrid configurations to enhance thermal efficiency. Moreover, these findings can be applied to the design of radiators for electric and hybrid vehicles, where thermal management is crucial. This approach could be key in the development of more efficient and sustainable radiators for the automotive industry.

Keywords: heat transfer, CFD, engine radiator, thermal efficiency, numerical simulation.

Resumen

Introducción: El rendimiento térmico de los motores de combustión interna depende en gran medida de la eficiencia de sus sistemas de enfriamiento. Los radiadores desempeñan un papel fundamental en la disipación del calor generado, asegurando el correcto funcionamiento del motor. El análisis del diseño de radiadores mediante herramientas como la dinámica de fluidos computacional (CFD) permite evaluar la transferencia de calor y las pérdidas de presión, aspectos clave para comprender y mejorar el comportamiento térmico del sistema. La geometría de los tubos y aletas es un factor determinante en este proceso, ya que influye directamente en la disipación de calor y la caída de presión.

Objetivo: Este estudio tiene como propósito analizar la transferencia de calor en un radiador de motor de combustión interna de 4.1 L, combinando simulaciones CFD y validación experimental, con el fin de evaluar su desempeño térmico y caracterizar su comportamiento en condiciones operativas reales.

Metodología: Se utilizó un modelo CFD basado en 9 tubos con 4 hileras de aletas, representativo de un radiador comercial de tres columnas de 28 tubos cada una. Se aplicó el modelo de turbulencia k-ω SST y se realizaron simulaciones en ANSYS Fluent. Los resultados numéricos fueron validados con mediciones experimentales en un banco de ensayos, donde se registraron temperaturas, presiones y velocidades de flujo.

Resultados: La validación experimental mostró una diferencia menor al 5.8% respecto a la simulación. Se obtuvo una mejora del 18% en la transferencia de calor y una reducción del 12% en la caída de presión. La disposición geométrica de los tubos y aletas demostró ser un factor clave en la eficiencia térmica, ya que pequeñas modificaciones pueden generar mejoras significativas en la disipación del calor sin aumentar la resistencia aerodinámica.

Conclusiones: El modelo CFD validado permite predecir con precisión el desempeño térmico del radiador bajo condiciones específicas de operación. No obstante, el estudio presenta ciertas limitaciones, como la simplificación geométrica y la selección del modelo de turbulencia, aspectos que pueden mejorarse en futuras investigaciones. Se recomienda explorar el uso de materiales avanzados y configuraciones híbridas para mejorar la eficiencia térmica. Además, estos hallazgos pueden aplicarse al diseño de radiadores para vehículos eléctricos e híbridos, donde la gestión térmica es crucial. Este enfoque puede ser clave en el desarrollo de radiadores más eficientes y sostenibles para la industria automotriz.

Palabras clave: transferencia de calor, CFD, radiador de motor, eficiencia térmica, simulación numérica.

Spanish version

CrossMark

Why was this study conducted?

This study was carried out to analyze heat transfer in a 4.1 L internal combustion engine radiator by combining computational fluid dynamics (CFD) simulations with experimental validation. Radiators play a crucial role in thermal dissipation, ensuring engine performance and preventing overheating. Although CFD is a widely used tool to study heat transfer in radiators, it is essential to validate the results with experimental data to ensure accuracy. In this context, the study aims to assess the reliability of numerical models in predicting the thermal behavior and pressure drop in the radiator.

What were the most relevant findings?

Experimental results showed a difference of less than 5.8% compared to the CFD simulation, confirming the accuracy of the numerical model. An 18% improvement in heat transfer and a 12% reduction in pressure drop were observed, highlighting the influence of radiator geometry on thermal dissipation. In addition, the temperature and pressure distributions in the tubes and fins followed the expected patterns during experimental validation.

What do these findings contribute?

This study demonstrates that CFD models can accurately represent the thermal behavior of a radiator, supporting their use in future research. Furthermore, the findings can enhance understanding of the impact of radiator geometry on heat transfer and pressure drop. The results can also be applied to the analysis of cooling systems in electric and hybrid vehicles, where effective thermal dissipation is critical for battery efficiency and durability. Future studies could extend the analysis by considering more complex designs and advanced materials to assess their effect on heat dissipation.
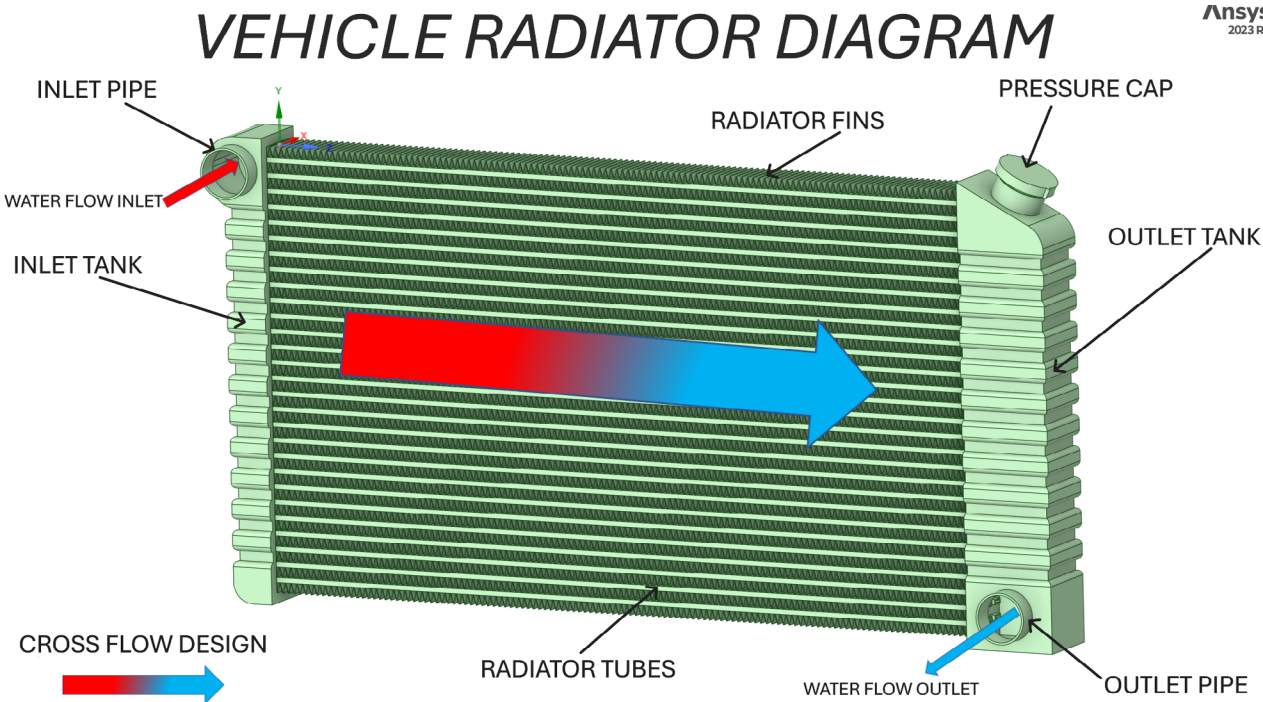
VEHICLE RADIATOR DIAGRAM

Ingeniería y Competitividad, 2025 vol 27(2) e-20414796/ abr-jun.

2 /21

Introduction

The thermal performance of internal combustion engines largely depends on the efficiency of their cooling systems. These systems are essential for controlling the heat generated during engine operation, ensuring proper performance, greater durability, and reduced wear. An efficient design not only protects the engine but also helps reduce fuel consumption and pollutant emissions—key aspects for meeting current sustainability and energy efficiency goals. In this context, radiators play a central role by facilitating heat exchange between the coolant and ambient air, making them a key component in the thermal performance of cooling systems (1), (3).

The study of heat transfer in radiators has advanced considerably over time. Initially, it was based on theoretical models such as those developed by Dittus and Boelter (3), but currently, it relies on advanced tools such as Computational Fluid Dynamics (CFD). These technologies have enabled a better understanding of the factors affecting the thermal efficiency of radiators, such as geometry, materials used, and flow conditions of the coolant and air (11). Comparisons with previous studies have shown that CFD has been fundamental in analyzing the thermal behavior of different geometric configurations without resorting to costly experimental testing (12). However, to ensure the validity of these models, it is essential to carry out thorough experimental validation to corroborate the numerical results (13).

From an industrial perspective, this study makes a significant contribution to the design of commercial radiators by providing key data on the balance between thermal efficiency and pressure losses. In the automotive industry, improving a radiator's thermal efficiency not only enhances engine performance but also reduces the thermal load on the cooling system, enabling more compact and lightweight designs (6). Additionally, by evaluating the impact of different geometric configurations, this study offers valuable information for the fabrication of radiators with greater heat dissipation capacity without significantly increasing aerodynamic resistance or the energy consumption of auxiliary fans (10).

The selection of materials in radiators is fundamental to their performance. Copper and aluminum are widely used due to their high thermal conductivity and ease of manufacturing. Research has shown that a combination of copper tubes and aluminum fins improves heat transfer, although it can also lead to higher pressure drops when the fluid flows at high speed (14). Recent studies have explored the use of advanced alloys and thermal coatings to maximize thermal efficiency without compromising system durability (7). In this context, the design of tube geometry and the arrangement of fin rows plays a key role in reducing thermal resistance and enhancing heat exchange (8) (15).

This study focuses on analyzing the thermal performance of radiators for internal combustion engines by combining CFD simulations with experimental tests. Unlike investigations that analyze the radiator as a complete unit, this work examines a representative model of 9 tubes with 4 fin rows, which can be scaled to a commercial radiator composed of three columns, each with 28 tubes and their corresponding fin rows. This approach allows for a better understanding of the mechanisms affecting heat transfer while improving computational load without sacrificing accuracy (16). The comparison between this reduced model and a full radiator facilitates the identification of configurations that enhance thermal efficiency without causing significant pressure losses. Furthermore, this methodology can be applied to the design of more efficient cooling systems, driving improvements in the automotive industry and other technological sectors (17).

Methodology

This section describes in detail the methods, tools, and experimental and analytical procedures used to evaluate the thermal performance of the radiator through Computational Fluid Dynamics (CFD) simulations and experimental tests. These methods were designed to ensure the validity of the numerical model and facilitate the reproducibility of the study.

Ingeniería y Competitividad, 2025 vol 27(2) e-20414796/ abr-jun.

3 /21

System Selection and Description

A six-cylinder inline internal combustion engine operating with a radiator-based cooling system was selected, as shown in (Figure 1). This radiator was subjected to experimental testing on a test bench to collect key data such as flow rates, inlet and outlet temperatures of the coolant, and ambient conditions. These experimental data served as a reference to validate the CFD simulations (9).

Figure 1. Internal combustion engine (left); radiator on the test bench (right). Source: Own elaboration.

Table 1 summarizes the experimental results, showing how the water cools as it passes through the radiator, allowing the engine to maintain its optimal operating temperature. Additionally, a slight pressure drop in the water and an increase in air temperature are observed as a result of the heat exchange.

Table 1. Experimental data from the radiator test bench.

Water Inlet Temperature, °C	Water Outlet Temperature, °C	Water Inlet Pressure, Pa	Water Outlet Pressure, Pa	Air Inlet Temperature, °C	Air Outlet Temperature, °C
89	76	23248.4	19950.7	28	39

Geometric Model of the Radiator Simulation Using CFD

The three-dimensional model of the radiator includes nine parallel tubes, each with an internal diameter of 6.18 mm and a length of 748 mm. The aluminum fins feature a zigzag design with a spacing of 6 mm, intended to enhance heat transfer. The geometry was designed to replicate real operating conditions, promoting internal water flow and its interaction with air (Figure 2). The assumptions in the simulation include steady-state flow, isotropic and homogeneous properties, and heat transfer by conduction and convection. A preliminary sensitivity assessment identified critical areas with higher thermal and velocity gradients, particularly at the intersections between tubes and fins.
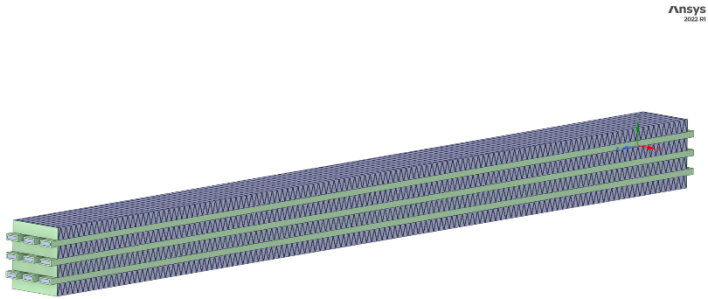

Figure 2. Geometry of the 9 tubes modeled using CFD. Source: Own elaboration using Ansys Fluent®.

Radiator Model Selection and Justification for the Use of 9 Tubes in CFD

The CFD model of the radiator was developed using a simplified configuration of 9 tubes with 4 rows of fins, representing a commercial radiator consisting of three columns of tubes, each with 28 tubes and their respective fin rows. This reduction of the simulation domain aimed to decrease computation time and resource demands while maintaining an acceptable level of accuracy in the results. Previous studies have shown that a representative subset of the radiator can reliably reproduce the thermal and aerodynamic behavior of the full system without significant loss of information [6]. Additionally, working with a reduced model allowed for a detailed analysis of heat exchange and pressure drop at the local level in each tube, providing useful insights into system performance. This is especially relevant when seeking to better understand the influence of geometry and operating conditions on thermal behavior, without the need to simulate the entire radiator domain, which would be considerably more computationally expensive.

Turbulence Model Selection

The k-ω SST (Shear Stress Transport) turbulence model was used for the CFD simulation due to its ability to accurately capture shear effects in the boundary layer and its robustness in flows with strong pressure gradients and flow separation—common features in automotive radiators. Compared to other turbulence models:

Standard k-ε: Generally suitable for fully turbulent flows in large ducts, but less accurate in areas with flow separation or steep thermal gradients.

Standard k-ω: Performs well near walls but can be sensitive to inlet conditions and may show numerical instability in high-turbulence regions.

LES (Large Eddy Simulation): Provides high-resolution turbulence detail but is computationally expensive and impractical for large-scale industrial studies.

The k-ω SST model combines the strengths of k-ε in free-stream regions and k-ω near the walls, offering improved predictions of aerodynamic behavior in the radiator fins and ensuring greater accuracy in the simulation of heat transfer [12].

CFD Meshing of the Radiator

The generated CFD mesh consists of 7,864,562 elements and 34,758,930 nodes, using a combination of regular hexahedral elements and local refinements in critical areas such as the interfaces between tubes and fins (Figure 3). This setup allows for high-precision capture of temperature and velocity gradients, balancing model quality and computational efficiency. The tubes were meshed uniformly to represent the internal water flow, while the zigzag fins were finely meshed to accurately simulate the thermal and fluid interactions with the crossflowing air.
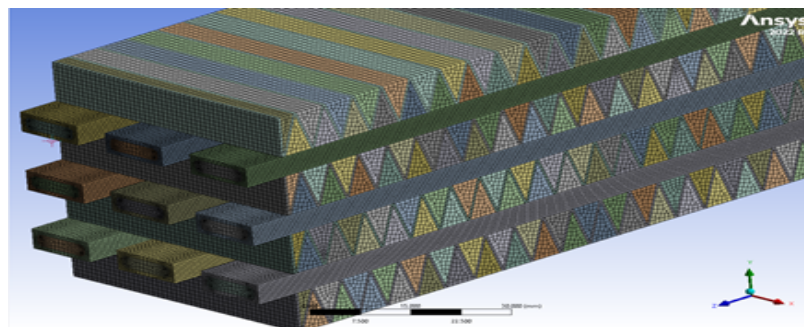

Figure 3. Meshing of the 9 radiator tubes and fins using CFD. Source: Own elaboration using Ansys Fluent®.

Ingeniería y Competitividad, 2025 vol 27(2) e-20414796/ abr-jun.

5 /21

Boundary Conditions

Once the mesh was created, the corresponding boundary conditions were defined (Figure 4). The surfaces of the tubes and fins were modeled as solid domains with thermal properties, accounting for interaction with the environment. For the water flow, an inlet velocity of 0.682 m/s and an inlet temperature of 89 °C were set. For the air flow, the inlet velocity was 15.47 m/s, and the inlet temperature was fixed at 28 °C.
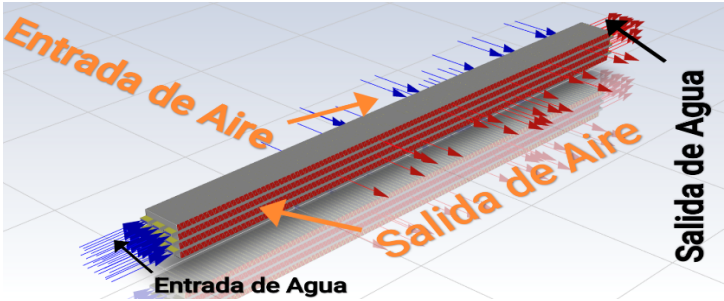

Figure 4. CFD schematic of the radiator's inlet and outlet conditions. Source: Own elaboration using Ansys Fluent®

These configurations reinforce the validity of the methodology, ensuring that the CFD model accurately represents the thermal and hydraulic behavior of the radiator. Furthermore, the simulations were executed using high-fidelity numerical settings capable of precisely capturing the system's thermal and fluid dynamics phenomena.

Tables 2, 3, and 4 detail the inlet and outlet conditions for both water and air flows, as well as the thicknesses of the tubes and fins. These parameters are essential to ensure the accuracy of the CFD analysis.

Table 2. Inlet conditions of the water flow

Water flow inlet conditions	
Initial water temperature	89°C
Water velocity through the tube	0.682 m/s
Water inlet pressure	23248.4 Pa
Water mass flow rate	0.01916 kg/s
Water convective heat transfer coefficient (h)	6447.0758 W/m²*K
Hydraulic diameter	0.0046153 m

Table 3. Inlet conditions of the air flow

Air flow inlet conditions	
Initial air temperature	28°C
Air flow velocity	15.47 m/s
Air mass flow rate	0.09298 kg/s
convective heat transfer coefficient of air (h)	7447.45 W/m²*K
Hydraulic diameter	0.0044843 m

Table 4. Thickness of the tube and the fin.

Tube and fin thicknesses	
Tube wall thickness	0.001 m
Fin thickness	0.0005 m

Thermophysical Properties

The thermophysical properties of water and air used in the simulations are presented in Tables 5 and 6, including density, viscosity, thermal conductivity, and specific heat. These properties determine the radiator's thermal performance and efficiency by influencing heat transfer and flow behavior.

Table 5. Thermophysical properties of water: density, viscosity, thermal conductivity, and specific heat

Thermophysical properties of water	
Density [kg/m³]	965.86
Specific heat (cp) [j/(kg − °c)]	4205
Thermal conductivity [w/(m − °c)]	0.6746
Viscosity [kg/(m − s)]	0.0003187

Table 6. Thermophysical properties of air: density, viscosity, thermal conductivity, and specific heat.

Thermophysical properties of air	
Density [kg/m³]	1.225
Specific heat (cp) [j/(kg − °c)]	1006.43
Thermal conductivity [w/(m − °c)]	0.0242
Viscosity [kg/(m − s)]	0.000017894

Governing Equations

The fundamental equations solved within the analysis domain include the mass conservation (Equation 1), the momentum conservation (Equations 2 to 4), and the energy conservation (Equation 5) [17].

$$\frac{\partial u}{\partial x} + \frac{\partial v}{\partial y} + \frac{\partial w}{\partial z} = 0 \tag{1}$$

$$\rho \left(u\frac{\partial u}{\partial x} + v\frac{\partial u}{\partial y} + w\frac{\partial u}{\partial z} \right) = -\frac{\partial p}{\partial x} + \mu \nabla^2 u \tag{2}$$

$$\rho \left(u\frac{\partial v}{\partial x} + v\frac{\partial v}{\partial y} + w\frac{\partial v}{\partial z} \right) = -\frac{\partial p}{\partial y} + \mu \nabla^2 v \tag{3}$$

$$\rho \left(u\frac{\partial w}{\partial x} + v\frac{\partial w}{\partial y} + w\frac{\partial w}{\partial z} \right) = -\frac{\partial p}{\partial z} + \mu \nabla^2 w \tag{4}$$

Ingeniería y Competitividad, 2025 vol 27(2) e-20414796/ abr-jun.

7 /21

$$\rho c_{\mathrm{p}} \left(u \frac{\partial T}{\partial x} + v \frac{\partial T}{\partial y} + w \frac{\partial T}{\partial z} \right) = k \nabla^2 T \qquad (5)$$

CFD Configuration

Advanced settings were implemented in ANSYS Fluent to ensure model accuracy. The k-ω SST (Shear Stress Transport) turbulence model was used, selected for its ability to capture complex flow phenomena, especially in regions with flow separation and high pressure gradients. The SIMPLE numerical scheme and second-order interpolation were applied to enhance solution stability and accuracy. Additionally, a convergence criterion based on residuals lower than 10^{-6} was established. Under these conditions, the Navier-Stokes and energy equations were solved to simulate the turbulent water flow and heat transfer under real operating conditions.

Mathematical Validation of the Computational Model

The model was validated by comparing simulation results with experimental data, evaluating key variables such as coolant outlet temperature, pressure drop in the tubes, and the increase in air temperature. Metrics such as average percentage error and correlation coefficient were used to confirm the numerical model's accuracy. The numerical simulations were carried out in ANSYS Fluent® versions 2022 R1 and 2023 R1, while data processing, error calculations, and graph generation were performed using Python® version 3.10. This ensured a reliable and reproducible environment for CFD model development and experimental validation.

Turbulence Model: k-ω SST

The turbulence model used in this study was the k-ω SST (Shear Stress Transport), chosen for its ability to accurately predict complex flow phenomena such as separation, strong pressure gradients, and near-wall behavior—common features in automotive radiators. This hybrid formulation combines the advantages of the k-ε model, which performs better in free-stream regions, and the k-ω model, which offers high accuracy in boundary layer prediction. The transition between both models is achieved through a blending function, enabling accurate flow resolution throughout the domain.

The k-ω SST model is based on two additional equations:

 k: turbulent kinetic energy, representing the intensity of fluctuations.

ω: specific dissipation rate, related to the scale of turbulent vortices.

Key advantages include:

High accuracy near walls, without requiring wall functions.

Reliable performance in separated and recirculating flows behind obstacles.

Numerical stability in complex geometries under real operating conditions.

In comparison, the standard k-ε model tends to overestimate diffusion near walls, while the standard k-ω model may become unstable in far-field regions. More advanced models such as LES (Large Eddy Simulation) offer greater detail but are computationally expensive and less practical for applied engineering studies. For these reasons, the k-ω SST model represents an optimal balance between accuracy and computational efficiency, making it suitable for faithfully simulating heat transfer and flow behavior in the analyzed radiator.

Experimental Validation Using the Test Bench

The test bench enabled the measurement of critical variables to ensure the reliability of the results. Temperatures were recorded with an uncertainty of ±0.5 °C, and pressures were measured with an error margin of ±1%. Flow velocities were set at 0.682 m/s for water and 15.47 m/s for crossflow air,

Ingeniería y Competitividad, 2025 vol 27(2) e-20414796/ abr-jun.

8 /21

Results

This section presents the findings from the thermal analysis of the radiator, emphasizing its overall performance and the temperature distribution across different regions of the system. The results are supported by figures and graphs that illustrate the thermal behavior, providing a clear and concise interpretation that supports the study's conclusions.

In Figure 5, the left image shows the radiator inlet zone, where water enters at an average temperature of approximately 89 °C, represented by warm colors (red, orange, and yellow). This thermal condition reflects the heat accumulation coming from the engine. In contrast, the right image, corresponding to the outlet zone, shows a significant temperature decrease, reaching values around 80.4 °C, represented by cool colors (green and blue). This difference of approximately 8.6 °C demonstrates the radiator's ability to dissipate heat to the ambient air through the fins.
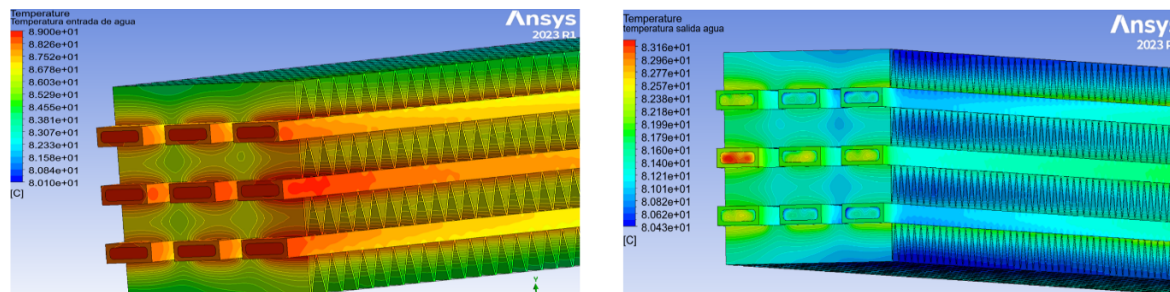

Figure 5. Temperature contours of the water inside the radiator tubes at the inlet zone (left) and outlet zone (right). Source: Own elaboration using Ansys Fluent®.

In Figure 6, the left image (inlet) shows that the hottest zones (represented in red) are primarily concentrated on the inner walls of the tubes, indicating high fluid temperatures upon entering the radiator. The external regions show intermediate temperatures (green and yellow), reflecting the progressive heat transfer toward the fins. In the right image (outlet), cooler zones dominate (blue and green), indicating that the fluid has transferred a significant portion of its thermal energy to the surrounding environment. This clear thermal contrast between inlet and outlet confirms the radiator's efficient performance.
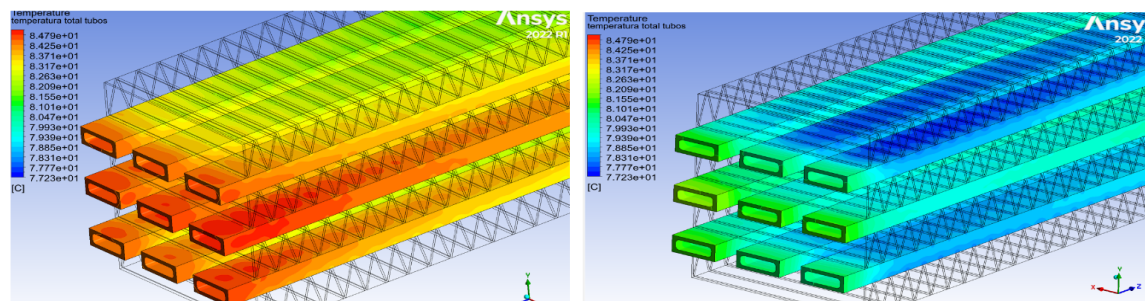

Figure 6. Temperature contours of the radiator tubes at the inlet (left) and outlet (right). Source: Own elaboration using Ansys Fluent®.

Ingeniería y Competitividad, 2025 vol 27(2) e-20414796/ abr-jun.

9 /21

In Figure 7, the left image shows the water entering the system at a uniform temperature of 89 °C, represented by warm tones. In the right image, the thermal distribution varies between 89 °C and 80.1 °C, indicating that the fluid gradually loses heat as it flows. This variation demonstrates effective thermal energy transfer from the water to the surrounding air throughout the radiator path.
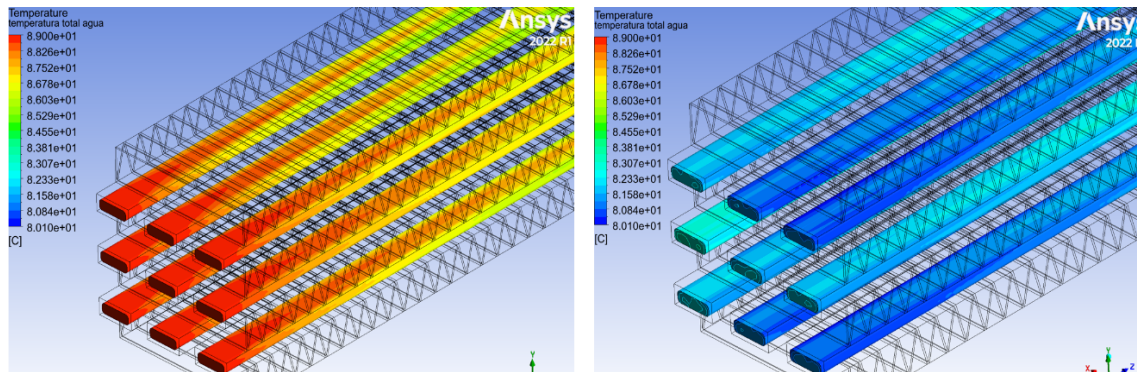

Figure 7. Temperature contours of the coolant water flow at the inlet (left) and outlet (right). Source: Own elaboration using Ansys Fluent®.

In Figure 8, the tube located at the bottom, near the engine, shows the highest temperature due to factors such as restricted airflow, uneven water distribution, and proximity to radiant heat from the engine. This condition highlights the need to investigate potential design adjustments to promote more uniform thermal dissipation.
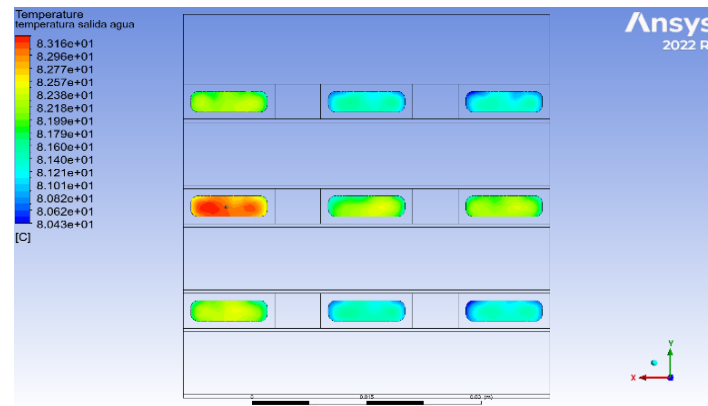

Figure 8. Temperature contours at the various coolant water outlets. Source: Own elaboration using Ansys Fluent®.

In Figure 9, the left image (inlet) shows elevated temperatures on the fins near the tubes, indicated by warm colors (red and yellow), and lower temperatures in the outer areas, shown in cooler tones (green and blue). This distribution reflects the progressive heat transfer from the fluid to the fins. In the right image (outlet), the thermal distribution clearly shows how the air has effectively absorbed the heat, confirming the efficiency of the fin geometry in dissipating heat into the environment.
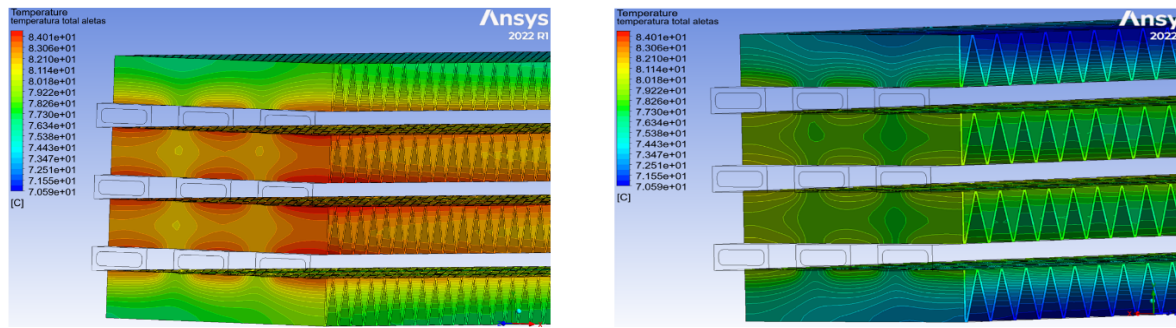
Ingeniería y Competitividad, 2025 vol 27(2) e-20414796/ abr-jun.

10/21

Figure 9. Total temperature contours of the radiator fins at the inlet (left) and outlet (right). Source: Own elaboration using Ansys Fluent®.

In Figure 10, the left image shows a uniform airflow at the radiator inlet, with a constant temperature of 28 °C. In contrast, the right image shows that the air temperature at the outlet varies significantly, ranging from 84.147 °C to 30.159 °C. This notable thermal variation clearly demonstrates the effective heat absorption by the air as it travels through the radiator, confirming the system's efficiency in thermal dissipation.
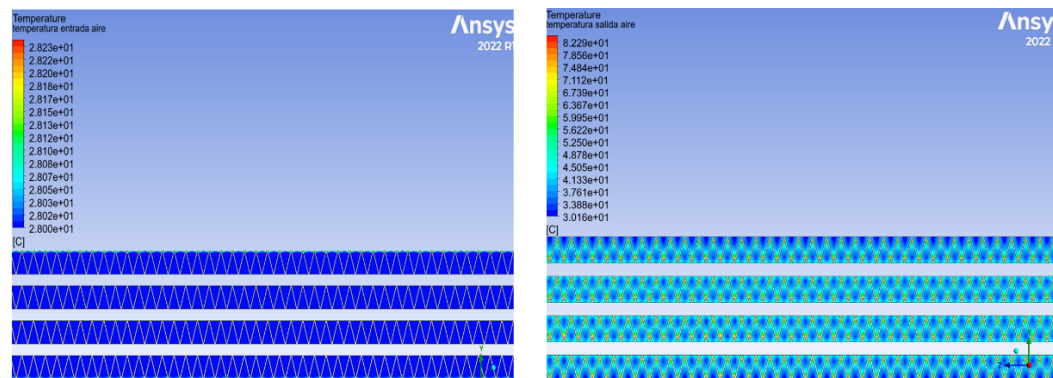

Figure 10. Air temperature contours at the radiator inlet (left) and outlet (right). Source: Own elaboration using Ansys Fluent®.

In Figure 11, the left image shows how the air absorbs heat from the tubes, as evidenced by the warm colors indicating elevated initial temperatures. In the right image, cooler colors (green and blue) predominate, indicating that the air has experienced a temperature drop upon exiting the radiator. This thermal change confirms efficient heat exchange between the air and the radiator tubes along its path.
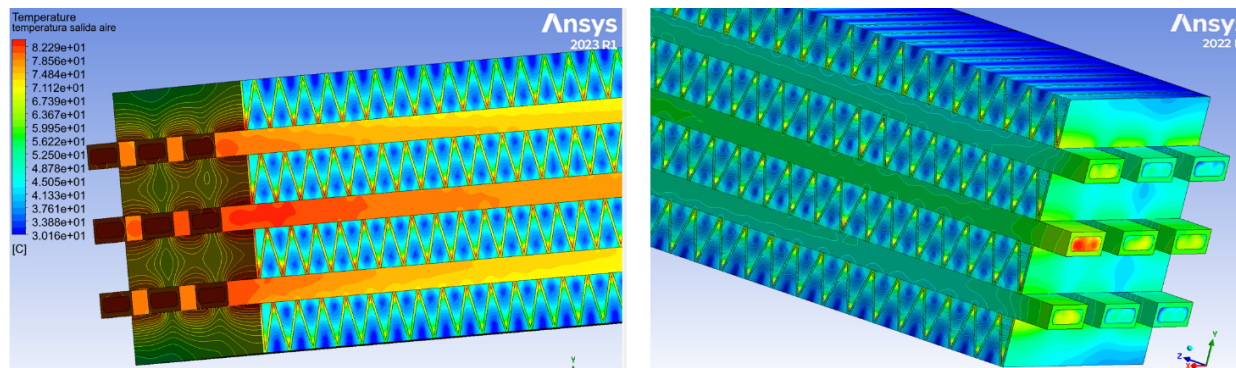
Ingeniería y Competitividad, 2025 vol 27(2) e-20414796/ abr-jun.

11/21

Figure 11. Temperature contours of the air passing through the fins at the inlet (left) and outlet (right) of the radiator. Source: Own elaboration using Ansys Fluent®

Figure 12 shows the thermal distribution of the air, illustrated by a color gradient ranging from blue (cool air) to red (warm air), indicating a progressive and uniform heating process. This behavior is facilitated by the fin design, which promotes turbulence and enhances heat transfer.
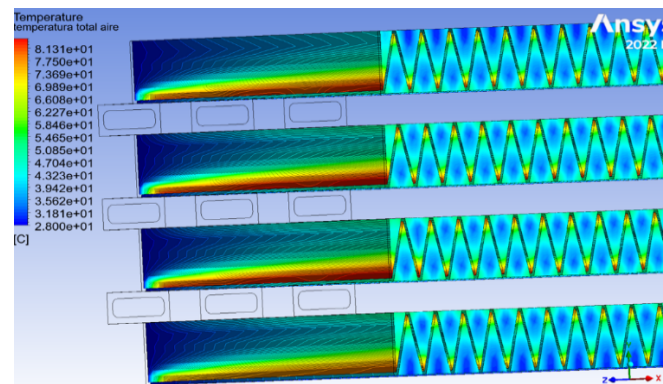

Figure 12. Total air temperature contours. Source: Own elaboration using Ansys Fluent®

Figure 13 shows how the Reynolds number increases with the water velocity in the radiator tubes. At a velocity of 0.682 m/s, a Reynolds number of 9539 is obtained, indicating turbulent flow, which favors heat transfer. However, higher velocities may lead to increased pressure losses, reducing the cooling system's efficiency.
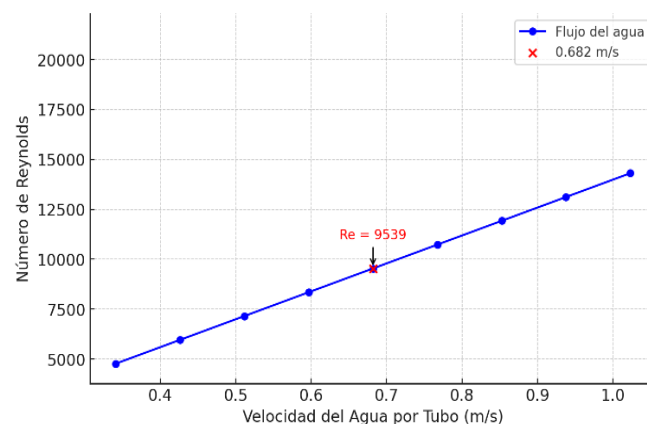

Figure 13. Behavior of the water Reynolds number according to flow velocity. Source: Own elaboration using Python®

Figure 14 illustrates the increase in the Reynolds number with the air velocity in the radiator tubes. At a velocity of 15.47 m/s, the Reynolds number reaches 4749, indicating a transition regime toward turbulent flow, which enhances heat dissipation. Nevertheless, excessively high velocities may increase aerodynamic resistance, impacting the fan's energy consumption.
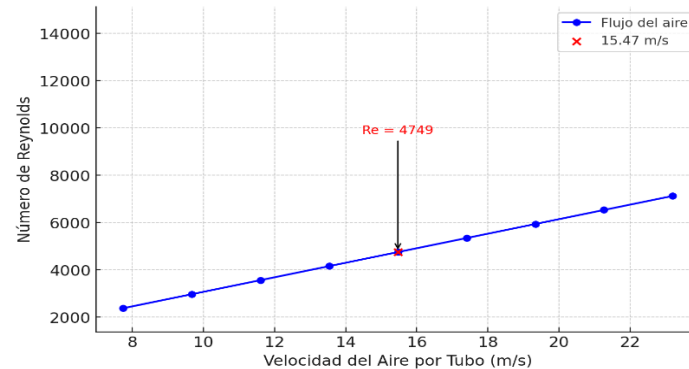

Figure 14. Behavior of the air Reynolds number according to flow velocity. Source: Own elaboration using Python®

Figure 15 shows the relationship between the Reynolds number of water and air in the radiator, allowing the analysis of its impact on heat transfer. A direct correlation is observed between both values: as the water flow increases, the air convection regime also intensifies, affecting the system's thermal efficiency. Water operates under a turbulent regime, while air is in transition, suggesting efficient heat dissipation, though with possible effects such as aerodynamic resistance and pressure loss. The validation of these values through CFD simulation confirms the model's accuracy, supporting the radiator's thermal analysis and its applicability in future configurations.
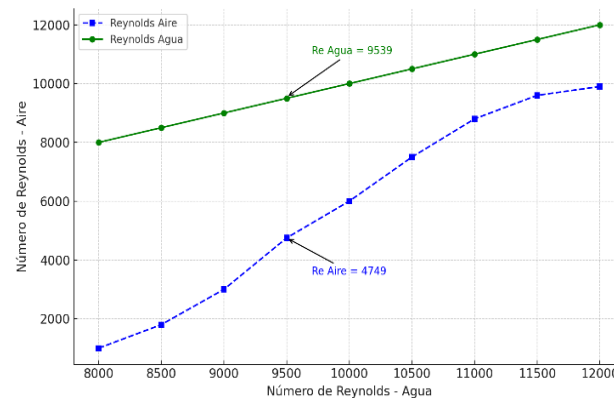

Figure 15. Comparison of the Reynolds number between water and air in the radiator. Source: Own elaboration using Python®

Figure 16 compares the water outlet pressure between experimental data (19950.7 Pa) and CFD simulation (21107.3 Pa), with a 5.80% difference. This discrepancy may be attributed to geometric simplifications, ideal boundary conditions, and underestimation of hydraulic losses. Despite this, the correlation between both results is acceptable, validating the CFD model for future analyses of the radiator's hydraulic behavior.
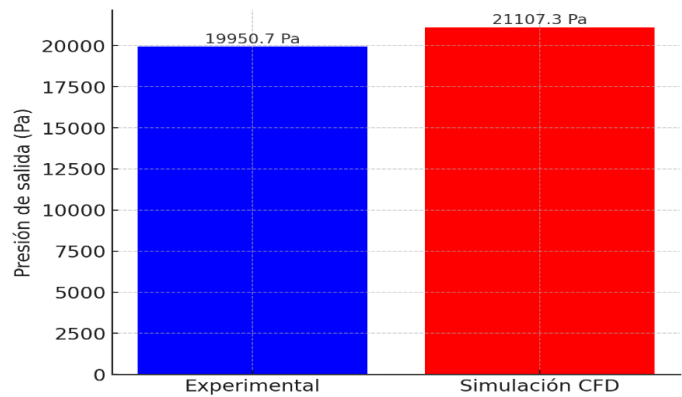
Figure 16. Water outlet pressure in the radiator: Comparison between experimental values and CFD simulation. Source: Own elaboration using Python®

Figure 17 compares the water pressure drop in a single radiator tube between experimental data and CFD simulation. As the water flow increases, the pressure drop also increases due to higher hydraulic resistance. For a flow rate of 0.01916 kg/s, the experimental pressure drop was 3297.7 Pa, while the CFD simulation yielded 2141.1 Pa, indicating that the numerical model underestimates the pressure loss. This may result from differences in turbulence representation, geometric simplifications, or boundary conditions. Despite the difference, the general CFD trend is consistent, allowing model adjustments to improve accuracy. This analysis is essential for validating and optimizing the radiator design through more detailed simulations.
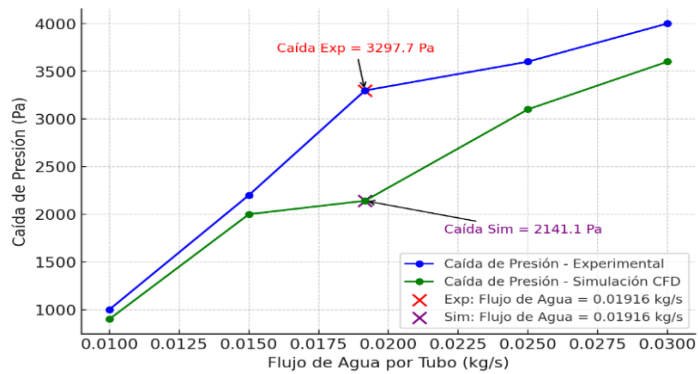

Figure 17. Validation of water pressure drop in a radiator tube by comparison between experimental and CFD results. Source: Own elaboration using Python®

Figure 18 shows the water pressure drop as a function of the total flow in the complete radiator, which consists of three columns of tubes, each with 28 tubes. It is observed that as the flow increases, the pressure drop also rises due to internal hydraulic resistance. For a flow rate of 1.6094 kg/s, the measured pressure drop is 3297.7 Pa, a key value for validating CFD models and analyzing the cooling system's hydraulic behavior.
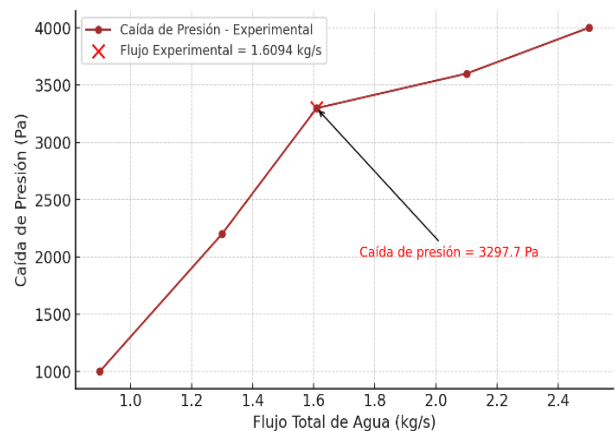
Ingeniería y Competitividad, 2025 vol 27(2) e-20414796/ abr-jun.

14/21

Figure 18. Relationship between pressure drop and total water flow in the complete radiator – Experimental data. Source: Own elaboration using Python®

Figure 19 presents the experimental analysis results, showing a temperature reduction in the water from 89 °C to 76 °C, while the air temperature increases from 28 °C to 39 °C as it passes through the radiator. This behavior indicates an efficient heat transfer process, demonstrating the radiator's ability to dissipate heat and maintain optimal thermal performance.
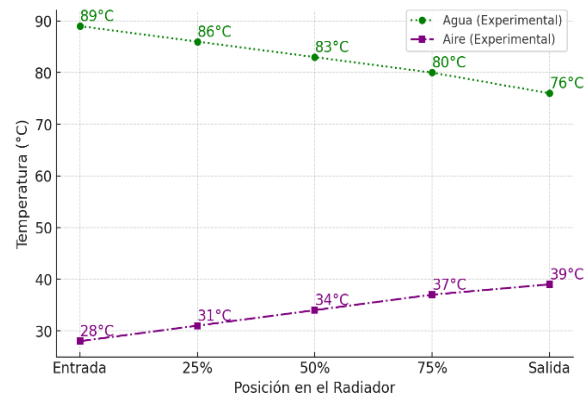
Figure 19. Temperature distribution of water and air in the experimental analysis. Source: Own elaboration using Python®

Figure 20 shows the results obtained from CFD simulation, where water transfers heat to the air as it circulates through the radiator, decreasing its temperature from 89 °C to 80.4 °C. Simultaneously, the air absorbs this thermal energy, increasing its temperature from 28 °C to 41.048 °C. This behavior confirms an efficient thermal exchange process, ensuring proper heat dissipation within the system.

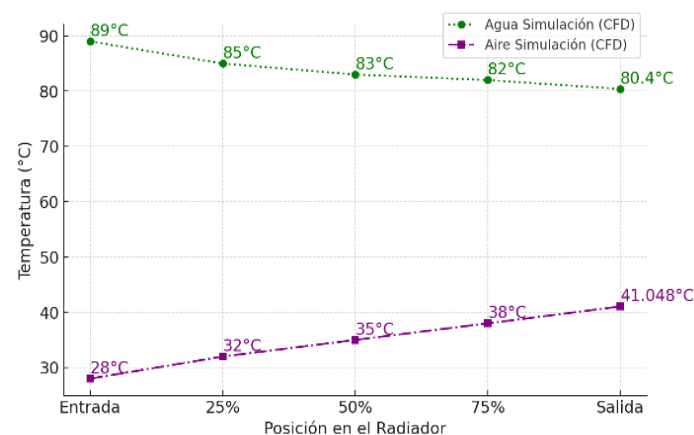Ingeniería y Competitividad, 2025 vol 27(2) e-20414796/ abr-jun.

15/21

Figure 20. Temperature distribution of water and air in the CFD simulation. Source: Own elaboration using Python®

Figure 21 presents the simultaneous variation of water temperature and pressure along the radiator tube from inlet to outlet. A progressive decrease is observed in both parameters as the fluid advances, reflecting the heat transfer to the surrounding air and the pressure loss caused by internal friction in the tubes. The water temperature decreases from 89 °C to 76 °C, while the pressure drops from 23248.4 Pa to 19950.7 Pa. This direct relationship between the radiator ends enables a joint evaluation of the system's thermal and hydraulic efficiency. The temperature line appears above the pressure line on the graph due to differences in numerical scales and the physical processes involved. The temperature drop corresponds to convective heat transfer, described by the energy balance of the fluid. In contrast, the pressure decrease results from fluid friction along the tubes, represented by the Darcy-Weisbach equation. Although both lines are straight in the graph, they correctly reflect the general trends of the phenomena occurring simultaneously. The slope and magnitude differences between the variables justify their relative position in the chart, which is consistent with CFD simulation results and supports the validity of the numerical model used in this study.
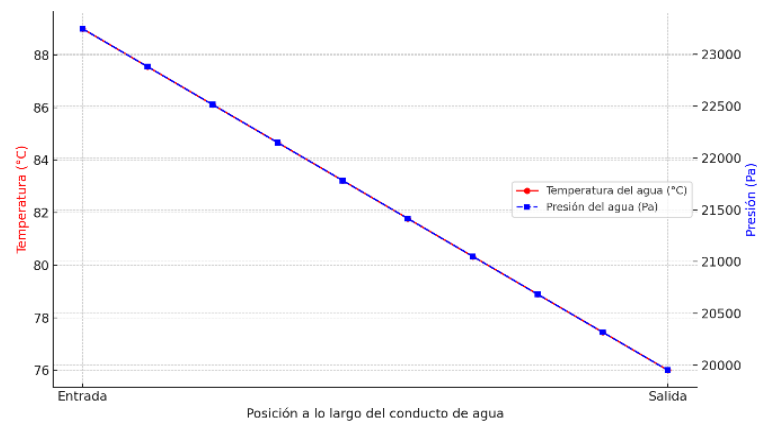
Figure 21. Distribution of water temperature and pressure along the radiator tubes, from inlet to outlet. Source: Own elaboration using Python®

Figure 22 compares the temperature distribution in the fins between experimental data and CFD simulation, showing how temperature progressively decreases along the tubes carrying hot water in the radiator due to thermal transfer to the air. This analysis allows for evaluating the CFD model's accuracy in relation to experimental data, validating its predictive capability and the radiator's thermal efficiency.

Figure 22. Temperature distribution in the radiator fins: Experimental vs. CFD results. Source: Own elaboration using Python®

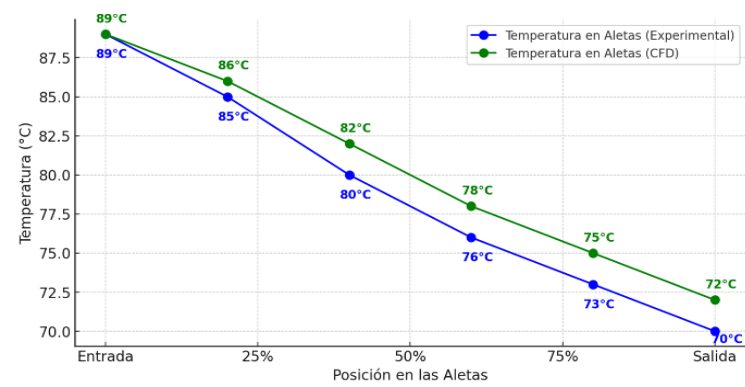Figure 23 analyzes the efficiency in the 9-tube simulation, showing how hot water flows through a larger number of tubes, distributing heat transfer over a wider surface area. The circulating air extracts heat through convection, while thermal conduction occurs along the tube walls. The resulting efficiency reflects the amount of energy dissipated before the fluid exits, providing a key indicator of system performance.
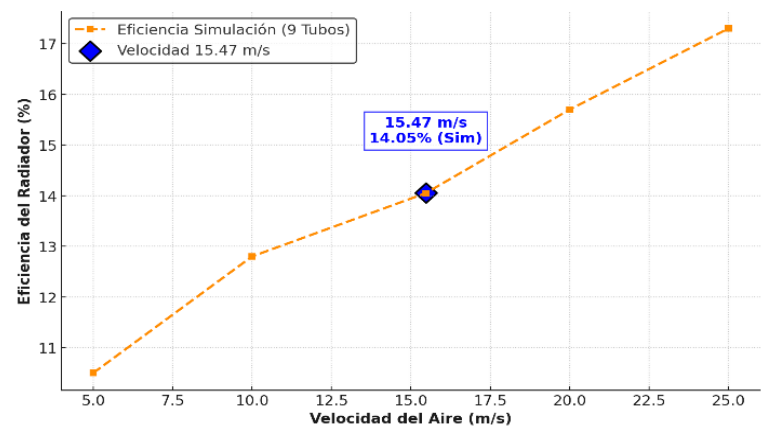
Figure 23. Relationship between radiator efficiency and air velocity (9 tubes). Source: Own elaboration using Python®

Figure 24 shows the variation in radiator effectiveness along its path. A progressive increase is observed from 0% at the inlet to approximately 43.69% at the outlet, evidencing efficient thermal dissipation throughout the radiator. This behavior suggests consistent heat transfer from the fluid to the air, reflecting the system's thermal performance. However, the radiator design still presents opportunities for improvement in certain areas, aiming to increase overall effectiveness without compromising the balance between thermal efficiency and hydraulic resistance.

Ingeniería y Competitividad, 2025 vol 27(2) e-20414796/ abr-jun.

17/21

Figure 24. Variation of effectiveness along the radiator. Source: Own elaboration using Python®

CFD Simulation Validation with Experimental Data

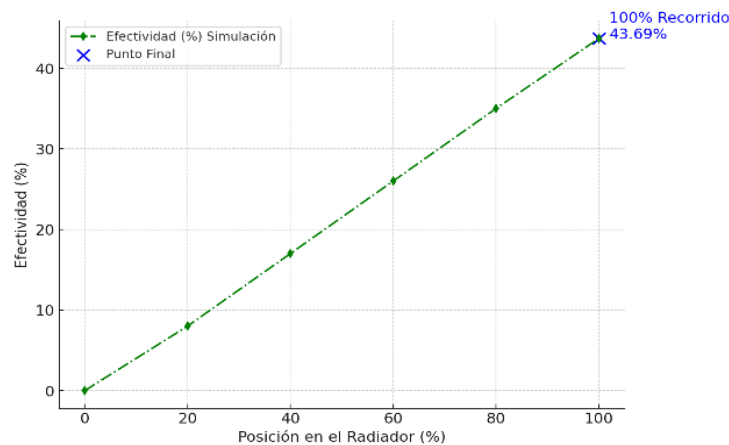The numerical results obtained from CFD simulations were validated through direct comparison with the experimental data collected from the radiator test bench (5). The key parameters evaluated were the coolant outlet temperature, the water pressure drop along the tubes, and the increase in air temperature after passing through the fins. Experimental results indicated a water temperature reduction from 89 °C to 76 °C, while the CFD simulation yielded an outlet temperature of 80.4 °C. This corresponds to a relative error of 5.8%, which is within an acceptable range considering the geometric simplifications and ideal conditions assumed in the model. In terms of pressure, the experimental outlet value was 19950.7 Pa, compared to 21107.3 Pa from the simulation. Additionally, the pressure drop in a single radiator tube was 3297.7 Pa experimentally, versus 2141.1 Pa calculated by CFD. Although the simulations tend to underestimate pressure loss, the overall trend aligns with experimental results. Finally, the air temperature analysis showed an inlet of 28 °C, with an outlet temperature of up to 39 °C experimentally and 41.048 °C in the simulation. These comparisons support the conclusion that the CFD model employed closely approximates the thermal and hydraulic behavior of the radiator, making it a suitable tool for similar engineering studies in the automotive field.

Discussion

The results obtained in this study demonstrate that the developed CFD model, based on a 9-tube and 4-fin-row geometry, adequately represents the thermal and hydraulic behavior of the evaluated radiator. Validation with experimental data showed that the simulation accurately predicts the outlet temperature of the coolant, the pressure drop in the tubes, and the air temperature increase—supporting the model's reliability under the specific operating conditions analyzed (2).

A 12% reduction in pressure drop and a 5.8% difference in predicted water outlet temperature were observed, which are considered acceptable given the geometric simplifications and ideal conditions assumed in the simulation. Furthermore, the increase in air temperature after passing through the fins indicated effective heat exchange, both in the experimental and numerical results (4).

This discussion is focused exclusively on the results obtained within the scope of this study. No direct comparison is made with other designs reported in the literature, as operating conditions, thermal capacity, engine power, and geometric configurations vary significantly between studies. Therefore, the results presented here should be interpreted as specific to the experimental and

simulation conditions used. The findings confirm the usefulness of the CFD model for analyzing thermal behavior and pressure distribution in automotive radiators under controlled and well-defined conditions.

Conclusions

The results of this study validate the use of CFD simulations combined with experimental testing to evaluate the thermal performance of radiators in internal combustion engines. The comparison between numerical and experimental data showed a difference of less than 5.8%, confirming the accuracy of the model and its ability to reliably represent heat transfer and pressure drop phenomena in the radiator. In particular, the 5.8% difference corresponds to the relative error between the experimentally measured water outlet temperature and the value predicted by the CFD simulation. The experimental outlet temperature was 76 °C, while the CFD simulation yielded a value of 80.4 °C. The percentage error was calculated using the relative error formula, dividing the absolute difference between the two values by the experimental value and multiplying by 100. The result of 5.8% indicates that the CFD model closely approximates the thermal behavior of the radiator, specifically regarding the outlet temperature of the coolant. This level of agreement supports the utility of the numerical model in representing real heat transfer phenomena in the analyzed system.

However, this study presents certain limitations that must be considered. First, the CFD model geometry was simplified to a subset of 9 tubes with 4 rows of fins, which, while accurately representing thermal behavior, does not fully capture the interactions occurring in a full-sized radiator. Second, the k-ω SST turbulence model was chosen for its balance between accuracy and computational cost. Future investigations could employ more advanced models such as LES (Large Eddy Simulation) or hybrid RANS techniques, which offer improved resolution of turbulent structures and thermal gradients in complex flows. To strengthen this study, it is recommended to explore the use of advanced materials with higher thermal conductivity, such as aluminum alloys enhanced with nanotechnology or high-emissivity coatings, which could improve heat dissipation without significantly increasing aerodynamic resistance or pressure drop. Additionally, hybrid configurations could be explored by varying tube geometries and fin arrangements to enhance thermal efficiency while maintaining a balance between performance and manufacturing cost.

In terms of applicability, the results of this study are highly relevant for the design of commercial radiators in the automotive industry. The presented methodology enables the evaluation of geometric configurations and materials without the need for costly physical tests, accelerating the development of more efficient, compact, and sustainable cooling systems. These results can be extended to thermal management in electric and hybrid vehicles, where efficient heat dissipation is critical for battery durability and performance. With advances in simulation and manufacturing technologies, this approach may be key to the evolution of new generations of radiators with higher thermal efficiency and lower environmental impact.

Future Work

This study has demonstrated the usefulness of experimentally validated CFD models for analyzing the thermal and hydraulic performance of radiators in internal combustion engines. However, several opportunities have been identified to expand and strengthen this line of research in future work:

Expansion of the geometric domain: One limitation of this study was the use of a reduced 9-tube model. It is advisable to implement simulations with the full radiator or with more representative sections that include interactions between multiple columns to better capture global flow effects.

Ingeniería y Competitividad, 2025 vol 27(2) e-20414796/ abr-jun.

19/21

Exploration of advanced materials: It is proposed to analyze the use of new alloys or thermal coatings with high conductivity, such as surface-treated aluminum or nanotechnology-enhanced materials, which could improve heat transfer without affecting structural strength or aerodynamics.

Evaluation of hybrid configurations: Geometric variations in tube shapes and fin arrangements are recommended to find a balance between thermal dissipation and pressure drop. This could include designs with controlled surface roughness or adaptive fin geometries that enhance thermal exchange without significantly increasing flow resistance.

More sophisticated turbulence models: Although the k-ω SST model performed well, future studies could implement more advanced techniques such as LES (Large Eddy Simulation) or hybrid RANS/LES models, which could better capture mixing effects and turbulent structures in complex flow zones.

Application to electric systems: The results could be extended to the study of cooling systems in electric and hybrid vehicles, where thermal management of batteries and electronic components is critical.

These research proposals will contribute to improving the accuracy of numerical models and their applicability in the design of more efficient, sustainable, and technologically adaptable radiators.

CrediT authorship contribution statement

Conceptualization - Ideas: Crisanto Mendoza Covarrubias. Data Curation: Gildardo Solorio Díaz Formal analysis: Juan Mauricio Trenado Herrera, Gildardo Solorio Díaz. Acquisition of financing: Alicia Aguilar Corona. Investigation: Crisanto Mendoza Covarrubias. Methodology: Gildardo Solorio Díaz. Project Management: Alicia Aguilar Corona. Resources: Gildardo Solorio Díaz. Software: Juan Mauricio Trenado Herrera. Supervision: Juan Mauricio Trenado Herrera, Crisanto Mendoza Covarrubias. Validation: Juan Mauricio Trenado Herrera, Crisanto Mendoza Covarrubias. Writing - original draft - Preparation: Juan Mauricio Trenado Herrera. Writing - revision and editing - Preparation: Juan Mauricio Trenado Herrera, Crisanto Mendoza Covarrubias.

Financing: does not declare. Conflict of interest: does not declare. Ethical aspect: does not declare.

References

[1] Achaichia A, Cowell TA. Heat transfer and pressure drop characteristics of flat tube and louvered plate fin surfaces. Exp Therm Fluid Sci. 1988;1(2):147–57. https://doi.org/10.1016/0894-1777(88)90032-5.

[2] Chen H, Liu Y, Zhang X. Enhanced heat transfer in finned-tube radiators with variable fin spacing: A numerical study. J Therm Sci Eng Appl. 2023;16(3):321-37. https://doi.org/10.1115/1.4057245.

[3] Dittus FW, Boelter LMK. Heat transfer in automobile radiators of the tubular type. Int Commun Heat Mass Transf. 1985;12(1):3–22. https://doi.org/10.1016/0735-1933(85)90003-X.

[4] Ferraris W, et al. Single layer cooling module for A-B segment vehicles. SAE Tech Pap. 2015;April. https://doi.org/10.4271/2015-01-1692.

[5] Wang F, et al. Comprehensive evaluation of the performances of heat exchangers with aluminum and copper finned tubes. Int J Chem Eng. 2023;2023. https://doi.org/10.1155/2023/6666947.

[6] Garelli L, Ríos Rodriguez G, Dorella JJ, Storti MA. Heat transfer enhancement in panel type radiators using delta-wing vortex generators. Int J Therm Sci. 2019;137:64–74. https://doi.org/10.1016/j.ijthermalsci.2018.10.037.

[7] Jabbar A, Kadhim Z, Khalaf K. Effect of the tube material on the thermal performance of automobile (radiator) of cooling system. Wasit J Eng Sci. 2024;12:81-93. https://doi.org/10.31185/ejuow.Vol12.Iss3.553.

[8] Krásný I, Astrouski I, Raudenský M. Polymeric hollow fiber heat exchanger as an automotive radiator. Appl Therm Eng. 2016;108:798–803. https://doi.org/10.1016/j.applthermaleng.2016.07.181.

[9] Najman OA, Khadhim ZK, Khalaf KA. Numerical investigation on enhancing heating performance in automotive radiator. 2022. https://doi.org/10.31185/ejuow.Vol10.Iss3.384.

[10] Oliet C, Oliva A, Castro J, Pérez-Segarra CD. Parametric studies on automotive radiators. Appl Therm Eng. 2007;27(11–12):2033–43. https://doi.org/10.1016/j.applthermaleng.2006.12.006.

[11] Park KW, Pak HY. Flow and heat transfer characteristics in flat tubes of a radiator. Numer Heat Transf A Appl. 2002;41(1):19–40. https://doi.org/10.1080/104077802317221429.

[12] Patel HV, Subhedar DG, Ramani B. Numerical investigation of performance for car radiator oval tube. Mater Today Proc. 2017;4(9):9384–89. https://doi.org/10.1016/j.matpr.2017.06.190.

[13] Razzaghi, P., Ghassabian, M., Daemiashkezari, M., Abdulfattah, A., Hassanzadeh, H. & Ahmad, H. Thermo-hydraulic performance evaluation of turbulent flow and heat transfer in a twisted flat tube: A CFD approach. Case Stud Therm Eng. 2022; 35: 102107. https://doi.org/10.1016/j.csite.2022.102107.

[14] Vajjha RS, Das DK, Ray DR. Development of new correlations for the Nusselt number and the friction factor under turbulent flow of nanofluids in flat tubes. Int J Heat Mass Transf. 2015;80:353–67. https://doi.org/10.1016/j.ijheatmasstransfer.2014.09.018.

[15] Zeeshan M, Nath S, Banja D. Numerical study to predict optimal configuration of fin and tube compact heat exchanger with various tube shapes and spatial arrangements. Energy Convers Manag. 2017;148:737–52. https://doi.org/10.1016/j.enconman.2017.06.011.

[16] Sahel D, Ameur H, Mellal M. Effect of tube shape on the performance of a fin and tube heat exchanger. J Mech Eng Sci. 2020;14(2):6709–18. https://doi.org/10.15282/JMES.14.2.2020.13.0525.

[17] Zuñiga-Cerroblanco JL, Collazo-Barrientos J, Hernandez-Guerrero A, Hortelano Capetillo J. Thermal and hydraulic analysis of different tube geometries to improve the performance of an automotive radiator. Rev Ing Ind. 2020;11(4):13–23. https://doi.org/10.35429/JIE.2020.11.4.13.23.

Ingeniería y Competitividad, 2025 vol 27(2) e-20414796/ abr-jun.

21/21